

Evaluation of lingual mucosa toxicity and recovery follow-up in rats, following sub-chronic exposure to titanium dioxide nanoparticles

Mohamed Shamel^{1,A–C,F}, Dina Rady^{2,3,C–F}, Mahmoud Al Ankily^{1,A–C,F}

¹ Department of Oral Biology, Faculty of Dentistry, British University in Egypt, Cairo, Egypt

² Department of Oral Biology, Faculty of Dentistry, Cairo University, Egypt

³ Stem Cells and Tissue Engineering Research Group, Faculty of Dentistry, Cairo University, Egypt

A – research concept and design; B – collection and/or assembly of data; C – data analysis and interpretation;

D – writing the article; E – critical revision of the article; F – final approval of the article

Dental and Medical Problems, ISSN 1644-387X (print), ISSN 2300-9020 (online)

Dent Med Probl. 2022;59(3):427–435

Address for correspondence

Dina Rady

E-mail: dina.radi@dentistry.cu.edu.eg

Funding sources

None declared

Conflict of interest

None declared

Acknowledgements

None declared

Received on February 14, 2021

Reviewed on April 22, 2021

Accepted on May 20, 2021

Published online on September 30, 2022

Abstract

Background. Nanosized titanium dioxide (TiO₂) particles are among the most widely used nanoparticles (NPs) worldwide due to their unique properties. The lingual mucosa is still neglected in terms of risk assessment with respect to the NP uptake.

Objectives. The aim of this study was to evaluate the effect of intragastric administration of TiO₂ NPs on the mucous membranes of the tongues of albino rats, as well as the potential benefits of a 4-week recovery period.

Material and methods. Twenty-one male albino rats were randomly divided into 3 groups ($n = 7$ per group). Group I served as a control group and received saline intragastrically daily for 30 days. The experimental groups included group II, which received TiO₂ NPs in the amount of 50 mg/kg of body weight (b.w.) intragastrically daily for 30 days, and group III, which also received TiO₂ NPs in the amount of 50 mg/kg b.w. intragastrically daily for 30 days, and then was allowed to recover for 4 weeks. Tongue specimens were collected for histological, immunohistochemical and morphometric examinations.

Results. The TiO₂ NP group II showed significant atrophic and degenerative changes in the tongue mucosa, which included reduced epithelial thickness in the ventral surface, with disfigurement in the filiform and fungiform papillae. Weak B cell lymphoma-2 (Bcl-2) immunoreactivity was also noted. The 4-week recovery group displayed improvement in the histological picture, with moderate to strong Bcl-2 immunoreactivity in the epithelial cell layers and the underlying connective tissue.

Conclusions. The use of TiO₂ NPs caused severe histological and apoptotic changes in the filiform and fungiform papillae, and the ventral surface of the tongue of the rats, while allowing recovery minimized the toxic effect of the NPs.

Keywords: titanium, titanium dioxide, nanoparticle, Bcl-2, rats

Cite as

Shamel M, Rady D, Al Ankily M. Evaluation of lingual mucosa toxicity and recovery follow-up in rats, following sub-chronic exposure to titanium dioxide nanoparticles. *Dent Med Probl.* 2022;59(3):427–435. doi:10.17219/dmp/137904

DOI

10.17219/dmp/137904

Copyright

Copyright by Author(s)

This is an article distributed under the terms of the

Creative Commons Attribution 3.0 Unported License (CC BY 3.0)

(<https://creativecommons.org/licenses/by/3.0/>).

Introduction

Continuous improvement in nanotechnology engineering has led to the extensive manufacturing and use of nanomaterials. Usually, nanomaterials are nano-sized solid particles with a diameter ranging from 1 nm to 100 nm. Among the popular metals and metal oxides occurring in the nanosized form are gold, silver, iron, and titanium oxide nanoparticles (NPs), which are widely used due to their superior physicochemical properties, such as optical features and magnetic activity, and high thermal and electrical conductivity. Another favorable characteristic is their large surface area to volume ratio.^{1,2} However, their escalating consumption raises concerns with regard to their impact on biological systems.³

Titanium dioxide nanoparticles (TiO₂ NPs) are widely used, as they exhibit unique properties, including antiviral, antibacterial and antifungal effects. Moreover, TiO₂ NPs are highly biocompatible, with great strength, corrosion resistance and low density.^{4,5} However, their specific large surface area and quantum effects increase their chemical reactivity in the human body. Strikingly, the incorporation of TiO₂ NPs in numerous products, such as food additives, cosmetics and dental care products, raises the exposure risk related to these NPs. Owing to their non-degradability and ability to accumulate in different tissues, elevated exposure to TiO₂ NPs may lead to chronic cytotoxicity.^{6,7}

Previously published research reports that TiO₂ NPs exert toxic effects on the human body. These include changes in the cell cycle, damage to the nuclear membrane and apoptosis.^{8,9} Additionally, it has been proposed that TiO₂ NPs might cause mitochondrial and DNA destruction within cells.^{10,11} The mechanism of TiO₂ NP toxicity can be summarized in 3 processes: (1) the production of reactive oxygen species (ROS)¹²; (2) damage to the cell wall and the lipid peroxidation of the cell membrane; and (3) the attachment of TiO₂ NPs to intracellular organelles and biological macromolecules, following damage to the cell membrane.¹³

Exposure to TiO₂ NPs can occur by many routes, including inhalation, injection, dermal and mucosal contact, and intragastric absorption. This can lead to the precipitation of TiO₂ NPs in different internal organs.^{14,15} Weir et al. reported that the highest amount of TiO₂ as nanosized particles <100 nm was found in candies and chewing gum.¹⁶ Thus, such products expose the oral mucosa to high doses of TiO₂.

The aim of the present study was to investigate the histopathological changes in the filiform and fungiform papillae, and the ventral surface of the tongue, following the intragastric administration of TiO₂ NPs in albino rats, as well as the possible effect of recovery after the withdrawal of the NPs.

Material and methods

Chemicals

Titanium dioxide NPs were purchased from Nano Gate, Cairo, Egypt. The TiO₂ powder consisted of 95–97% anatase phase and 3–5% brookite phase, with NPs of an average size of 15 ± 3 nm and a spherical shape (based on transmission electron microscopy (TEM)). The TiO₂ anatase particles were prepared by precipitation from a homogeneous solution, using titanium (IV) isopropoxide as a precursor in an aqueous solution acidified with nitric acid to a pH of 2, with a water-to-titanium mole ratio of about 200.¹⁷

Animals

Twenty-one male albino rats weighing 150–200 g were used in the study. The rats were 2 months old, which is equivalent to the age of a human child. Children are susceptible to consuming up to 4 times more TiO₂/kg of body weight (b.w.) as compared to adults.¹⁸

Experimental protocol

The experiment was conducted according to the guidance and approval of the Ethical Committee at the Faculty of Dentistry of Ain Shams University, Cairo, Egypt (approval No.: 615/2017).

The animals were provided by and housed in the Animal Research Center of Ain Shams University. The animals were housed in a sterile, controlled environment, with a temperature of 25 ± 2°C and 12-hour dark/light cycles. They were kept in individual cages, with 5 rats per cage. The size of the cage was 20 cm in width and 40 cm in length. The cages were cleaned on a daily basis, and the rats were allowed free access to food and water. Each rat was given a unique number. The rats were randomly and equally allocated into 3 main groups ($n = 7$):

- group I: the rats received saline intragastrically daily for 30 days to serve as controls;
- group II: the rats received TiO₂ NPs in the amount of 50 mg/kg b.w. intragastrically daily for 30 days¹⁹; and
- group III: the rats received TiO₂ NPs in the amount of 50 mg/kg b.w. daily for 30 days as in group II, and were then allowed to recover for 4 weeks after treatment.

The rats were euthanized with an intracardiac overdose of sodium thiopental (80 mg/kg b.w.), following the different experimental periods.²⁰

Postmortem specimen processing

The rats' tongues were excised and fixed immediately in 10% phosphate-buffered formaldehyde solution for 48 h. The specimens were washed adequately under run-

ning water, dehydrated by transferring through a series of graded alcohol, cleared in xylene, and embedded in paraffin wax according to the standard technique.²¹

Hematoxylin and eosin staining

Longitudinal sections, 5-micron-thick, were obtained. The right sides of the tongues were stained with hematoxylin and eosin (H&E).²¹ A light microscope (Leica, Wetzlar, Germany) with $\times 400$ magnification was used to obtain images that were transferred to a computer system for analysis. The epithelial thicknesses of the filiform and fungiform papillae, and the ventral surface of the tongue were measured (in microns) using the ImageJ software, v. 1.41a (National Institutes of Health (NIH), Bethesda, USA; <https://imagej.nih.gov/ij/>).

Immunohistochemical staining

The left sides of the tongue tissue specimens (formalin-fixed and paraffin-embedded) were used for anti-active B cell lymphoma-2 (Bcl-2) localization.²² The polyclonal primary rabbit anti-active Bcl-2 supplied by Biocare Medical (Pacheco, USA) (1:100 in phosphate-buffered saline (PBS)), code No. CP 229 A, was applied. All sections were counterstained with hematoxylin, incubated for 2–3 min, rinsed in distilled water, dehydrated in graded alcohol, and cleared in xylene. Finally, the specimens were mounted by using an aqueous mounting medium, cover slips were put in place and the samples were examined with a light microscope.

For immunohistochemical evaluation, the Bcl-2-stained cell surface area percentage was measured using the ImageJ software, v. 1.41a.

Statistical analysis

The mean (M) and standard deviation (SD) values for the epithelial thickness (μm) and the Bcl-2 mean area percentage were analyzed using the IBM SPSS Statistics for Windows software, v. 26.0 (IBM Corp., Armonk, USA). The one-way analysis of variance (ANOVA) and Student's t test were used to compare the data. A p -value equal to or less than 0.05 was considered statistically significant.

Results

Histopathological results (H&E staining)

Filiform papillae

Group I (control)

The control group specimens showed a normal dorsum surface of the tongue with abundant slender filiform papillae that were regularly arranged and covered with keratinized stratified squamous epithelium. These papillae presented a uniform arrangement of the epithelial cell layers, and the keratin layer was evident. There were dispersed clear cells. The underlying lamina propria revealed normal cellular and fibrous elements, and appeared to merge with the subjacent tongue muscles without a clear line of demarcation (Fig. 1A).

Group II (TiO₂ NPs)

As compared to group I, there was noticeable disfigurement in the structure of the filiform papillae, with a marked reduction in their height; they exhibited blunt-ended tops.

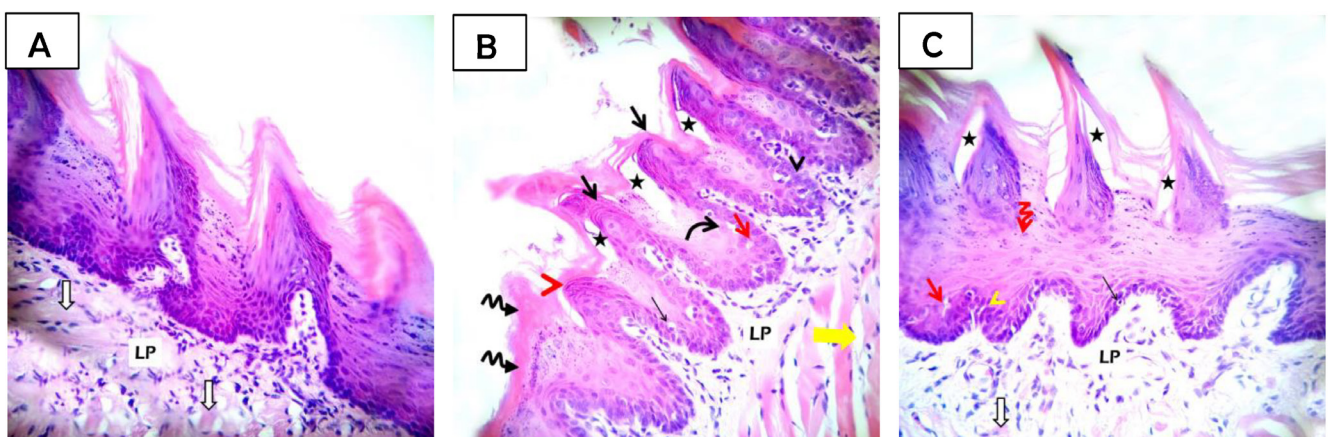


Fig. 1. Photomicrographs of the dorsal surface of the rat tongue, demonstrating the filiform papillae (hematoxylin and eosin (H&E), $\times 400$ magnification)

A – group I showing normal, cone-shaped keratinized filiform papillae with a normal architecture of the lamina propria (LP) and tongue muscles (white arrows); B – group II showing disfigured papillae with blunt-ended tops (black arrows), a short papilla (red arrow head), the loss of the papillae with hyperkeratosis (wavy black arrows), the loss of the papillae with evident hyperkeratosis (curved black arrow), focal areas of separation in the keratin layer (black stars), the epithelium with basilar hyperplasia (black arrow head), cytoplasmic vacuolation (red arrow), clear cells (thin black arrow), inflammatory cell infiltrate in the lamina propria (LP), and separation between muscle fibers (yellow arrow); C – group III showing the papillae seemingly regaining their normal appearance; still, with the epithelium revealing mild basilar hyperplasia (yellow arrow head), binucleated cells (curved red arrow), cytoplasmic vacuolation (red arrow), clear cells (thin black arrow), focal areas of separation in the keratin layer (black stars), and inflammatory cell infiltrate in the lamina propria (LP), white arrow – muscle fibers.

Also, some areas revealed a complete loss of the papillae with evident hyperkeratosis. Focal separation of the keratin layer from the underlying epithelial cells was also observed. The basal cell layer appeared disorganized, with basilar hyperplasia and some nuclear alterations in the form of pyknosis. Some of the basal and suprabasal epithelial cells had vacuolated cytoplasm. Numerous clear cells were recognized. The lamina propria showed signs of degeneration, with moderate inflammatory cell infiltration. Separation between tongue muscle fibers was noted (Fig. 1B).

Group III (TiO₂ NPs with 4-week recovery)

The tongues of the rats that were allowed a recovery period of 4 weeks after 30 days of TiO₂ NP induction were similar to those in the control group in the histological picture of the surface epithelium and the lamina propria. The epithelium appeared to have a considerable thickness and a regular basement membrane. The basal cell layer exhibited mild basilar hyperplasia and large hyperchromatic nuclei. The prickle cell layer displayed a few binucleated cells. The granular cells exhibited distinct keratohyalin granules, but a few cells appeared with vacuolation. The keratin layer was irregular, had nonuniform thickness in certain areas, and had focal areas of separation. A few clear cells were identified throughout the epithelial layers. The underlying lamina propria showed less degenerative areas, deeply stained basophilic fibroblasts and a small number of inflammatory cells (Fig. 1C).

Fungiform papillae

Group I (control)

The fungiform papillae were of normal mushroom shape and were composed of normal stratified squamous epithelium with a thin uniform layer of keratin and a vascular connective tissue core. A single barrel-shaped taste bud with peripherally arranged cells was observed on the

upper surface of the papillae. Lingual muscle fibers ran in different directions (Fig. 2A).

Group II (TiO₂ NPs)

The fungiform papilla was shorter and distorted, and showed signs of epithelial atrophy. Atrophic changes in the shape and orientation of the taste bud cells, which were separated, were also observed. Atrophy in the connective tissue and tongue musculature was noted (Fig. 2B).

Group III (TiO₂ NPs with 4-week recovery)

Similar to the control group, the fungiform papillae assumed a mushroom-like appearance, with almost normal epithelial covering and a barrel-shaped taste bud with normal cells. Reduced signs of degeneration within the lamina propria and the blood vessels engorged with blood cells were observed. Lingual muscle fibers appeared to run in different directions (Fig. 2C).

Ventral surface of the tongue

Group I (control)

The mucous membrane of the ventral surface of the tongue had a regular, thin keratin layer that lacked the lingual papillae. The lamina propria was formed of the connective tissue. Muscle fibers were composed of the interlacing bundles running in different directions (Fig. 3A).

Group II (TiO₂ NPs)

The ventral surface of the tongue showed the atrophy of the surface epithelium, observed as a reduction in the thickness of the surface epithelium. An apparent loss of the keratin layer was observed. The dissociation of the collagen fibers of the lamina propria and congested blood vessels were noted. Skeletal muscle fibers were apparently atrophied and separated (Fig. 3B).

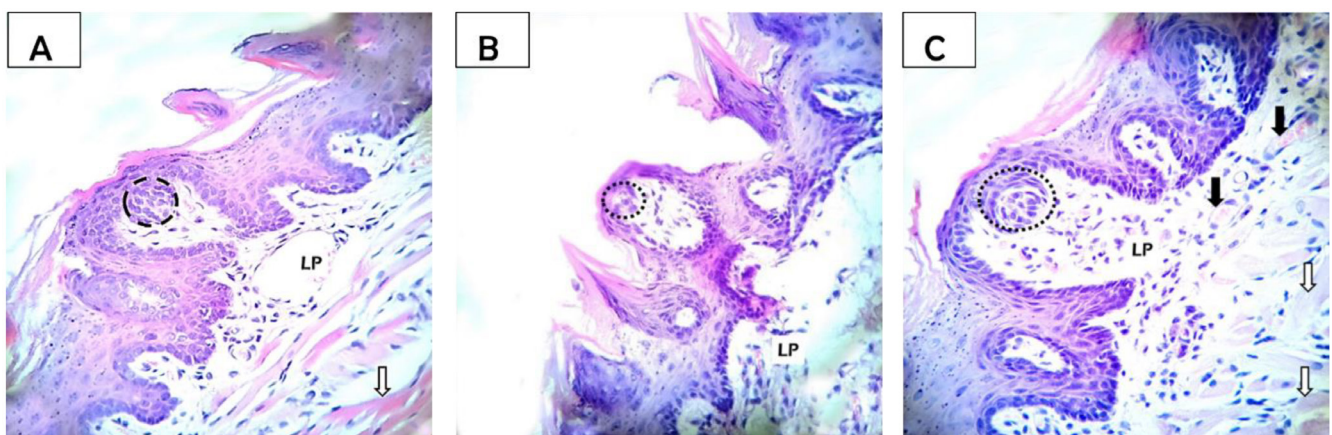


Fig. 2. Photomicrographs of the dorsal surface of the rat tongue, demonstrating the fungiform papillae (hematoxylin and eosin (H&E), ×400 magnification)

A – group I showing a normal mushroom shape of the papilla with a normal barrel-shaped taste bud (dotted circle), LP – lamina propria, white arrow – muscle fibers; B – group II showing the distortion of the papilla with signs of atrophy in a taste bud (dotted circle) and the lamina propria (LP); C – group III showing a nearly normal shape of the papillae and a taste bud with almost a regular arrangement of taste cells (dotted circle), the lamina propria (LP), blood vessels (black arrows), and muscle fibers (white arrows).

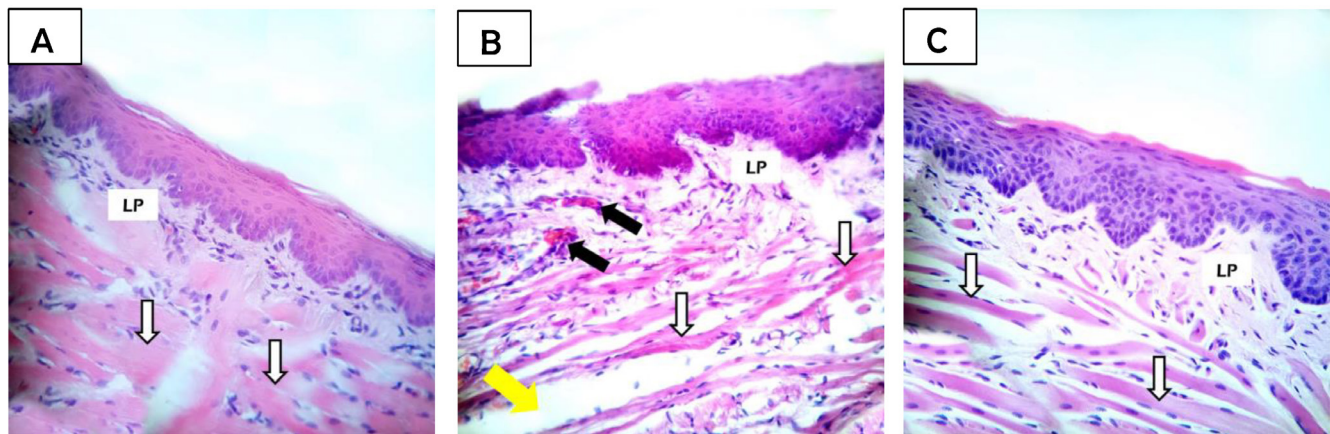


Fig. 3. Photomicrographs of the ventral surface of the rat tongue (hematoxylin and eosin (H&E), x400 magnification)

A – group I showing no lingual papillae and the presence of a regular, thin keratin layer, LP – lamina propria, white arrows – muscle fibers; B – group II showing an irregular contour with thin epithelium, the loss of the keratin layer, congested blood vessels (black arrows), and atrophied muscle fibers (white arrows) with separation between muscle fibers (yellow arrow), LP – lamina propria; C – group III showing the presence of normal epithelium with a thin keratin layer, muscle fibers (white arrows) and the lamina propria (LP).

Group III (TiO₂ NPs with 4-week recovery)

The ventral surface of the tongue regained its normal surface epithelium thickness, with a thin keratin layer and a normal pattern of epithelial ridges. Lingual muscle fibers ran in different directions (Fig. 3C).

Morphometric analysis

Statistical analysis for the mean epithelial thickness of the filiform and fungiform papillae, and the ventral surface of the tongue in the 3 groups is presented in Tables 1 and Tables 2.

The ANOVA revealed statistically significant differences between the 3 groups in the mean epithelial thickness of the filiform and fungiform papillae, and the ventral surface of the tongue ($p < 0.01$). The highest mean epithelial thickness of the filiform and fungiform papillae, and the ventral surface of the tongue was recorded in group I (control), whereas the lowest mean epithelial thickness was recorded in group II (TiO₂ NPs).

The pairwise comparison conducted with the use of unpaired Student's t test revealed a statistically significant decrease in the mean epithelial thickness of the filiform and fungiform papillae, and the ventral surface of the tongue in group II (TiO₂ NPs) as compared to both group I (control) and group III (TiO₂ NPs with 4-week recovery) ($p < 0.01$).

Table 1. Epithelial thickness [μm] of the filiform and fungiform papillae, and the ventral surface of the tongue in the 3 examined groups

Group	Filiform papillae	Fungiform papillae	Ventral surface of the tongue
I	364.03 ± 8.81	202.59 ± 7.28	118.20 ± 13.20
II	163.19 ± 12.41	128.77 ± 5.79	61.63 ± 5.80
III	356.83 ± 5.09	196.34 ± 2.40	108.50 ± 6.70

Data presented as mean ± standard deviation ($M \pm SD$).

Table 2. Pairwise comparison between the examined groups with regard to the mean epithelial thickness [μm] of the filiform and fungiform papillae, and the ventral surface of the tongue

Variables	Comparison	MD	p -value
Filiform papillae	group I vs. group II	200.84	<0.010*
	group I vs. group III	7.20	0.090
	group II vs. group III	193.64	<0.010*
Fungiform papillae	group I vs. group II	73.82	<0.010*
	group I vs. group III	6.25	0.052
	group II vs. group III	67.57	<0.010*
Ventral surface of the tongue	group I vs. group II	56.57	<0.010*
	group I vs. group III	9.70	0.100
	group II vs. group III	46.87	<0.010*

MD – mean difference; * statistically significant.

Immunohistochemical results

The immunostained sections obtained from the filiform and fungiform papillae, and the ventral surface of the tongue of group I showed numerous cells with positive Bcl-2 immunoreactivity, indicating a strong reaction affecting the epithelial layers and extending to the underlying connective tissue cells in the form of brownish coloration (Fig. 4A, 5A and 6A). The Bcl-2-immunostained sections of group II demonstrated a marked reduction in positively stained cells, indicating a weak reaction (Fig. 4B, 5B and 6B). The Bcl-2-immunostained sections of group III revealed a moderate-to-strong reaction in the epithelial cell layers and the underlying connective tissue (Fig. 4C, 5C and 6C).

Morphometric analysis

Statistical analysis for the mean percentage of the area of the cells positively stained with Bcl-2 immune stain in all groups for the different examined specimens is shown in Tables 3 and Tables 4.

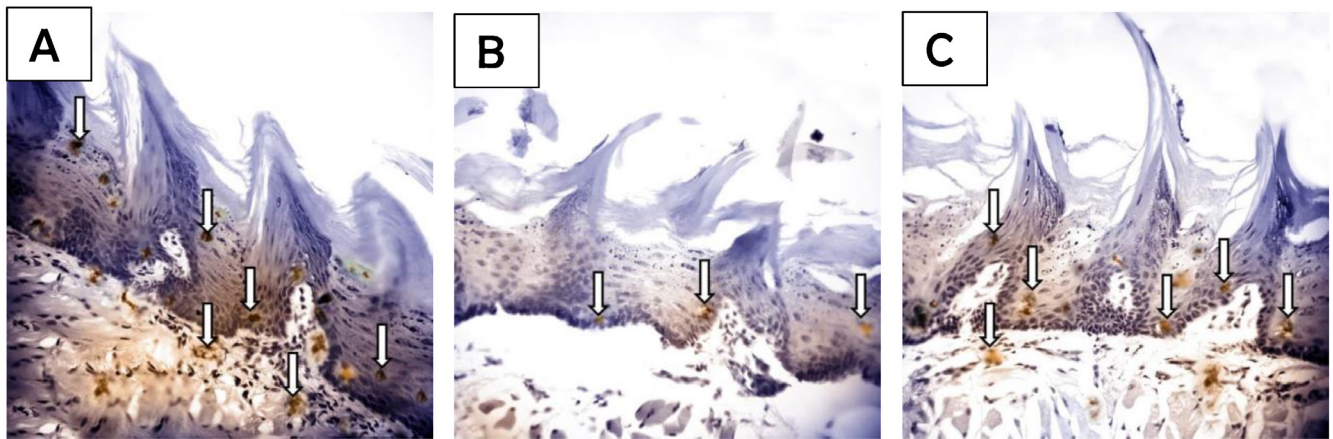


Fig. 4. Photomicrographs of the dorsal surface of the rat tongue, demonstrating the filiform papillae (B cell lymphoma-2 (Bcl-2), ×400 magnification)

A – group I showing a strong cytoplasmic reaction to Bcl-2 in several epithelial layers and the underlying connective tissue; B – group II showing a negative cytoplasmic reaction in most epithelial cells except for few positive cells; C – group III showing a moderate-to-strong cytoplasmic reaction to Bcl-2 in the basal cell layer, which is evident in some prickles, with few positive cells in the connective tissue. White arrows indicate positively stained cells.

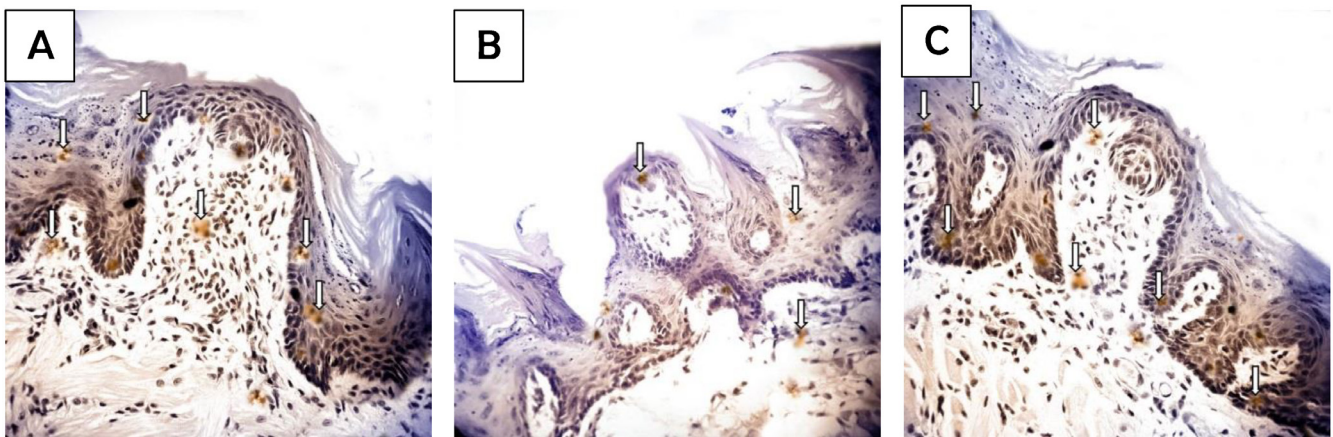


Fig. 5. Photomicrographs of the dorsal surface of the rat tongue, demonstrating the fungiform papillae (B cell lymphoma-2 (Bcl-2), ×400 magnification)

A – group I showing a strong cytoplasmic reaction to Bcl-2 in the basal and suprabasal cell layers, and the underlying connective tissue; B – group II showing a negative cytoplasmic reaction except for few positive cells; C – group III showing a moderate-to-strong cytoplasmic reaction to Bcl-2. White arrows indicate positively stained cells.

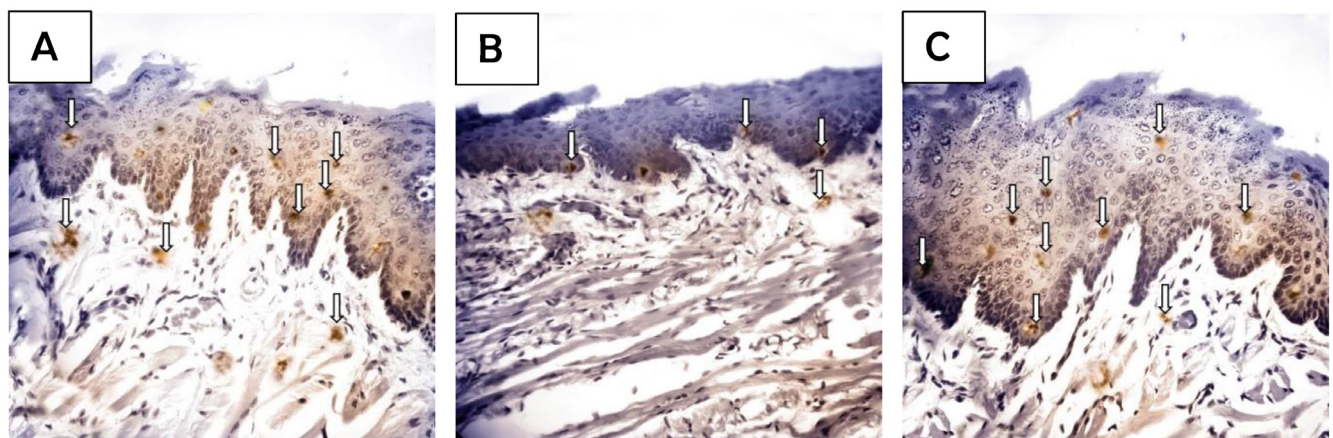


Fig. 6. Photomicrographs of the ventral surface of the rat tongue (B cell lymphoma-2 (Bcl-2), ×400 magnification)

A – group I showing a strong cytoplasmic reaction to Bcl-2 in the epithelial layers and the underlying connective tissue; B – group II showing a weak reaction, mainly in the basal cell layer and the underlying connective tissue; C – group III showing a moderate-to-strong cytoplasmic reaction to Bcl-2 in all epithelial layers and the underlying connective tissue. White arrows indicate positively stained cells.

Table 3. B cell lymphoma-2 (Bcl-2)-stained cell surface area percentage in the filiform and fungiform papillae, and the ventral surface of the tongue in the 3 examined groups

Group	Filiform papillae	Fungiform papillae	Ventral surface of the tongue
I	32.49 ±0.90	32.54 ±1.32	37.18 ±0.52
II	12.24 ±0.96	14.06 ±1.31	24.62 ±0.83
III	31.46 ±0.97	31.14 ±1.31	36.60 ±0.46

Data presented as $M \pm SD$.

Table 4. Pairwise comparison between the examined groups with regard to the mean B cell lymphoma-2 (Bcl-2)-stained cell surface area percentage in the filiform and fungiform papillae, and the ventral surface of the tongue

Variables	Comparison	MD	p-value
Filiform papillae	group I vs. group II	20.25	<0.010*
	group I vs. group III	1.03	0.060
	group II vs. group III	19.22	<0.010*
Fungiform papillae	group I vs. group II	18.48	<0.010*
	group I vs. group III	1.40	0.070
	group II vs. group III	17.08	<0.010*
Ventral surface of the tongue	group I vs. group II	12.56	<0.010*
	group I vs. group III	0.58	0.060
	group II vs. group III	11.98	<0.010*

* statistically significant.

The ANOVA displayed statistically significant differences between the 3 groups ($p < 0.01$), with the highest mean Bcl-2-stained cell surface area percentage in the filiform and fungiform papillae, and the ventral surface of the tongue observed in group I (control), and the lowest mean area percentage recorded in group II (TiO₂ NPs).

The pairwise comparison conducted with the use of unpaired Student's *t* test revealed a statistically significant decrease in the mean Bcl-2-stained cell surface area percentage in the filiform and fungiform papillae, and the ventral surface of the tongue in group II (TiO₂ NPs) as compared to both group I (control) and group III (TiO₂ NPs with 4-week recovery) ($p < 0.01$).

Discussion

Titanium dioxide NPs are extensively and frequently utilized in many fields of industry, which increases the risk of exposure and gives rise to serious controversies about their potential effects on the human body. Hence, understanding the effects of TiO₂ NPs on biological systems is essential for the development of safe nanotechnology.

Even though TiO₂ NPs have been considered inert and nontoxic, and are among the most often used NPs, there is increasing evidence suggesting the contrary. Generally, the cytotoxic effects of TiO₂ NPs are accompanied by cell growth inhibition in different cell types.^{8,23,24} With the growing use of TiO₂ NPs in the food industry and

dentistry, as shown in several studies,²⁵ there is an urgent need to evaluate the histopathological changes in the lingual mucosa following the administration of TiO₂ NPs in albino rats, as well as possible recovery after their withdrawal.

The TiO₂ administration methods and doses assessed in rats are variable. In this study, the rats received TiO₂ NPs at a dose of 50 mg/kg b.w. per day intragastrically for 30 days as subchronic exposure.¹⁹ The intake of dietary TiO₂ NPs in the United Kingdom has been estimated to be about 5 mg/person/day,²⁶ which is equivalent to approx. 0.1 mg/kg b.w. per day.²⁷ In this study, 500 × the estimated human exposure dose (50 mg/kg b.w.) was used as low-dose TiO₂ NP exposure.

Intragastric administration was the route of choice in this study. Previous studies investigated the capacity of TiO₂ NPs to cross biological barriers, such as the gastrointestinal tract. Weir et al. provided evidence that TiO₂ NPs can pass from the gastrointestinal tract through the circulation to the lungs, spleen, liver, and kidneys up to 2 weeks after exposure.²⁸ Moreover, even when the dose was low, orally administered TiO₂ NPs (5, 50 and 500 mg/kg b.w.) accumulated in mice permanently, which caused inflammation, apoptosis and oxidative stress, and consequently gave rise to chronic gastritis.²⁹

The TiO₂ powder with an average size of NPs of 15 ±3 nm, consisting of 95–97% anatase phase and 3–5% brookite phase was used in this study. Jin et al. reported that TiO₂ NPs with a diameter <25 nm in the anatase crystalline phase caused genotoxicity.³⁰ In comparison with rutile and brookite, anatase has more industrial applications, but it is the most toxic form.³⁰

Usually, the shape of the particle plays a key role in the accumulation of TiO₂ NPs in the tissue and cellular response.^{31,32} In this study, TiO₂ NPs were spherical in shape. An in vitro study demonstrated a correlation between the shape of TiO₂ NPs and cell penetration.³³ Titanium dioxide NPs penetrated into normal reconstituted human buccal epithelium, with the sphere-shaped NPs found deeper in the epithelium as compared to the spindle-shaped ones.³³ This might be explained by the lower cellular uptake being associated with a high aspect ratio, in which it takes longer for the cell membrane to wrap around the elongated particles.³⁴

The light microscopic findings of this study clearly revealed that the administration of TiO₂ NPs caused evident structural changes in the tongue mucosa of the rats (Fig. 1B, 2B and 3B). These changes included atrophied filiform papillae, with an alteration in their normal height and number. They exhibited blunt-ended tops, with a total or partial loss of their characteristic conical shape, and evident hyperkeratosis. Moreover, the fungiform papillae were shrunk and displayed malformed architecture with degenerated taste buds. Similarly, the ventral surface of the tongue displayed atrophied epithelium with an apparent loss of the keratin layer.

This cytotoxic effect of TiO₂ NPs on the tongue mucosa might be mediated by oxidative stress, as reported in an in vitro study.¹⁰ Human hepatocellular cells were exposed to TiO₂ NPs at a concentration of 250 mg/mL, which caused an increase in ROS levels up to two-fold at 5-hour exposure duration, thereby causing DNA damage.¹⁰ An in vivo investigation revealed nuclear shrinkage and chromatin condensation in the nuclei of neurons as well as the DNA ladder in the hippocampus of mice as a result of TiO₂ NP deposition; these features are considered the classical characteristics of apoptosis.³⁵

Strikingly, there were areas devoid of the lingual papillae on the dorsal surface of the tongue. This might also be due to a direct effect on the genetic constituents of cells, whereby TiO₂ NPs were able to induce DNA strand breaks and genetic instability.³⁶ Thus, it could be expected that the widespread use of TiO₂ NPs in many products leads to repeated exposure, which might exhaust the proliferative capability of the epithelium, and ultimately lead to epithelial atrophy.³³

Occasional inflammatory cell infiltration was observed in the lamina propria of the tongues of the rats exposed to TiO₂ NPs, which might designate the activation of the defense mechanism.^{37,38} Parallel results were observed in animals exposed to TiO₂ NPs in other studies; they exhibited inflammation in the tissues of the kidneys and liver.^{37,39} Moreover, in the present study, congested blood vessels were noticed (Fig. 3B). This coincides with an in vivo study, which determined that the intraperitoneal injection of TiO₂ NPs created capillary congestion and hemorrhage in the alveolar wall, which resulted from ROS generation.⁴⁰

There was remarkable atrophy and separation in the underlying tongue musculature; this is consistent with the findings of Wang et al., who reported damage in cardiac muscles after 30 days of oral exposure to TiO₂ NPs (0, 10, 50, 200 mg/kg b.w. per day).⁴¹ This muscular damage was further correlated to disrupted levels of proinflammatory cytokines and transcription regulators in the hearts of mice.⁴²

In group III (TiO₂ NPs with 4-week recovery), the histological findings (Fig. 1C, 2C and 3C) revealed similar results to those in group I (control) (Fig. 1A, 2A and 3A). The epithelium appeared to have a considerable thickness, with a regular basement membrane, and the underlying lamina propria showed fewer degenerative areas. These results are consistent with those of El-Sheikh et al., who reported moderate improvement in the histopathological changes in rat spleens after the administration of TiO₂ NPs was ceased for 8 weeks.⁴³

There was a significant decrease in the mean epithelial thickness in group II (TiO₂ NPs) as compared to both group I and group III ($p < 0.01$ and $p < 0.01$, respectively). The fact that the epithelial thickness was almost back to normal after the recovery period, despite the marked atrophy, indicates notable basal cell proliferation to compensate for this cell loss. Desquamation is one of the most efficient processes by which the stratified squamous epithelium of the body eliminates potentially harmful agents.⁴⁴

The immunohistochemical results showed a statistically significant decrease in the mean Bcl-2 area percentage expressed in group II (TiO₂ NPs) as compared to group I (control) and group III (TiO₂ NPs with 4-week recovery) ($p < 0.01$, $p < 0.01$, respectively). Hu et al. clearly demonstrated that hippocampal apoptosis in response to TiO₂ NP exposure significantly reduced Bcl-2 expression in the hippocampus of mice.³⁵ Thus, they concluded that TiO₂ NP-induced apoptosis in the mouse hippocampus was primarily mediated through the intrinsic apoptosis pathway.³⁵

Conclusions

Our research suggests that a low dose and extended exposure duration, which mimics the potential human exposure to TiO₂ NPs, can lead to cytotoxic effects on the lingual mucosa of albino rats. These cytotoxic effects could be moderately improved by discontinuing the administration of TiO₂ NPs for a period of time. We recommend increasing the period of discontinuation, as complete improvement may occur. In this sense, it is important that people who consume food containing engineered TiO₂ NPs for long periods of time should be particularly concerned. Moreover, our data suggests that the oral cavity should be the subject of TiO₂ NP risk assessment studies in the future.

Ethics approval and consent to participate

The experiment was conducted according to the guidance and approval of the Ethical Committee at the Faculty of Dentistry of Ain Shams University, Cairo, Egypt (approval No.: 615/2017).


Data availability

The datasets generated and/or analyzed during the current study are available from the corresponding author on reasonable request.


Consent for publication

Not applicable.

ORCID iDs

Mohamed Shamel  <https://orcid.org/0000-0003-0061-5163>

Dina Rady  <https://orcid.org/0000-0002-9672-6935>

Mahmoud Al Ankily  <https://orcid.org/0000-0002-8935-4619>

References

1. Banfield JF, Zhang H. Nanoparticles in the environment. *Rev Mineral Geochem.* 2001;44(1):1–58. doi:10.2138/rmg.2001.44.01
2. Aderibigbe BA. Metal-based nanoparticles for the treatment of infectious diseases. *Molecules.* 2017;22(8):1370–2017. doi:10.3390/molecules22081370

3. Nel A, Xia T, Madler L, Li N. Toxic potential of materials at the nano-level. *Science*. 2006;311(5761):622–627. doi:10.1126/science.1114397
4. Gupta SM, Tripathi M. A review of TiO₂ nanoparticles. *Chin Sci Bull*. 2011;56(16):1639–1657. doi:10.1007/s11434-011-4476-1
5. Ortlieb M. White giant or white dwarf?: Particle size distribution measurements of TiO₂. *GIT Lab J Europe*. 2010;14:42–43.
6. Hong J, Zhang YQ. Murine liver damage caused by exposure to nano-titanium dioxide. *Nanotechnology*. 2016;27(11):112001. doi:10.1088/0957-4484/27/11/112001
7. Shi H, Magaye R, Castranova V, Zhao J. Titanium dioxide nanoparticles: A review of current toxicological data. *Part Fibre Toxicol*. 2013;10:15. doi:10.1186/1743-8977-10-15
8. Acar MS, Bulut ZB, Ateş A, Nami B, Koçak N, Yıldız B. Titanium dioxide nanoparticles induce cytotoxicity and reduce mitotic index in human amniotic fluid-derived cells. *Hum Exp Toxicol*. 2015;34(1):74–82. doi:10.1177/0960327114530742
9. Coccini T, Grandi S, Lonati D, Locatelli C, De Simone U. Comparative cellular toxicity of titanium dioxide nanoparticles on human astrocyte and neuronal cells after acute and prolonged exposure. *Neurotoxicology*. 2015; 48:77–89. DOI: 10.1016/j.neuro.2015.03.006
10. Petković J, Zegura B, Stevanović M, et al. DNA damage and alteration in expression of DNA damage responsive genes induced by TiO₂ nanoparticles in human hepatoma HepG2 cells. *Nanotoxicology*. 2011;5(3):341–353. doi:10.3109/17435390.2010.507316
11. Baranowska-Wójcik E, Szwajgier D, Oleszczuk P, Winiarska-Mieczan A. Effects of titanium dioxide nanoparticles exposure on human health – a review. *Biol Trace Elem Res*. 2020;193(1):118–129. doi:10.1007/s12011-019-01706-6
12. Aillon KL, Xie Y, El-Gendy N, Berkland CJ, Forrest ML. Effects of nanomaterial physicochemical properties on in vivo toxicity. *Adv Drug Deliv Rev*. 2009;61(6):457–466. doi:10.1016/j.addr.2009.03.010
13. Hou J, Wang L, Wang C, et al. Toxicity and mechanisms of action of titanium dioxide nanoparticles in living organisms. *J Environ Sci (China)*. 2019;75:40–53. doi:10.1016/j.jes.2018.06.010
14. Bahadar H, Maqbool F, Niaz K, Abdollahi M. Toxicity of nanoparticles and an overview of current experimental models. *Iran Biomed J*. 2016;20(1):1–11. doi:10.7508/ibj.2016.01.001
15. Song B, Zhang Y, Liu J, Feng X, Zhou T, Shao L. Is neurotoxicity of metallic nanoparticles the cascades of oxidative stress? *Nanoscale Res Lett*. 2016;11(1):291. doi:10.1186/s11671-016-1508-4
16. Weir A, Westerhoff P, Fabricius L, Hristovski K, von Goetz N. Titanium dioxide nanoparticles in food and personal care products. *Environ Sci Technol*. 2012;46(4):2242–2250. doi:10.1021/es204168d
17. Powell JJ, Faria N, Thomas-McKay E, Pele LC. Origin and fate of dietary nanoparticles and microparticles in the gastrointestinal tract. *J Autoimmun*. 2010;34(3):J226–J233. doi:10.1016/j.jaut.2009.11.006
18. Musiał J, Krakowiak R, Mlynarczyk DT, Goslinski T, Stanisław BJ. Titanium dioxide nanoparticles in food and personal care products – what do we know about their safety? *Nanomaterials (Basel)*. 2020;10(6):1110.
19. Chen Z, Wang Y, Zhuo L, et al. Effect of titanium dioxide nanoparticles on the cardiovascular system after oral administration. *Toxicol Lett*. 2015;239(2):123–130. doi:10.1016/j.toxlet.2015.09.013
20. Rady D, Mubarak R, Abdel Moneim RA. Healing capacity of bone marrow mesenchymal stem cells versus platelet-rich fibrin in tibial bone defects of albino rats: An in vivo study. *F1000Res*. 2018;7:1573. doi:10.12688/f1000research.15985.1
21. Bancroft JD, Layton C. The hematoxylin and eosin. In: Suvarna S, Layton C, Bancroft JD eds. *Bancroft's Theory and Practice of Histological Techniques*. 7th ed. Philadelphia, PA: Churchill Livingstone/Elsevier; 2013:173–186.
22. Ozer H, Yenicesu G, Arici S, Cetin M, Tuncer E, Cetin A. Immunohistochemistry with apoptotic-antiapoptotic proteins (p53, p21, bax, bcl-2), c-kit, telomerase, and metallothionein as a diagnostic aid in benign, borderline, and malignant serous and mucinous ovarian tumors. *Diagn Pathol*. 2012;7:124. doi:10.1186/1746-1596-7-124
23. Armand L, Biola-Clier M, Bobyk L, et al. Molecular responses of alveolar epithelial A549 cells to chronic exposure to titanium dioxide nanoparticles: A proteomic view. *J Proteomics*. 2016;134:163–173. doi:10.1016/j.jprot.2015.08.006
24. Wang J, Ma J, Dong L, et al. Effect of anatase TiO₂ nanoparticles on the growth of RSC-364 rat synovial cell. *J Nanosci Nanotechnol*. 2013;13(6):3874–3879. doi:10.1166/jnn.2013.7145
25. Ziental D, Czarczynska-Goslinska B, Mlynarczyk DT, et al. Titanium dioxide nanoparticles: Prospects and applications in medicine. *Nanomaterials (Basel)*. 2020;10(2):387. doi:10.3390/nano10020387
26. Skocaj M, Filipic M, Petkovic J, Novak S. Titanium dioxide in our everyday life; is it safe? *Radiol Oncol*. 2011;45(4):227–247. doi:10.2478/v10019-011-0037-0
27. Chen Z, Wang Y, Ba T, et al. Genotoxic evaluation of titanium dioxide nanoparticles in vivo and in vitro. *Toxicol Lett*. 2014;226(3):314–319. doi:10.1016/j.toxlet.2014.02.020
28. Wang J, Zhou G, Chen C, et al. Acute toxicity and biodistribution of different sized titanium dioxide particles in mice after oral administration. *Toxicol Lett*. 2007;168(2):176–185. doi:10.1016/j.toxlet.2006.12.001
29. Hamad Mohamed HR. Estimation of TiO₂ nanoparticle-induced genotoxicity persistence and possible chronic gastritis-induction in mice. *Food Chem Toxicol*. 2015;83:76–83. doi:10.1016/j.fct.2015.05.018
30. Jin C, Tang Y, Yang FG, et al. Cellular toxicity of TiO₂ nanoparticles in anatase and rutile crystal phase. *Biol Trace Elem Res*. 2011;141(1–3):3–15. doi:10.1007/s12011-010-8707-0
31. Duan X, Li Y. Physicochemical characteristics of nanoparticles affect circulation, biodistribution, cellular internalization, and trafficking. *Small*. 2013;9(9–10):1521–1532. doi:10.1002/smll.201201390
32. Fubini B, Ghiazza M, Fenoglio I. Physico-chemical features of engineered nanoparticles relevant to their toxicity. *Nanotoxicology*. 2010;4:347–363. doi:10.3109/17435390.2010.509519
33. Konstantinova V, Ibrahim M, Lie SA, et al. Nano-TiO₂ penetration of oral mucosa: In vitro analysis using 3D organotypic human buccal mucosa models. *J Oral Pathol Med*. 2017;46(3):214–222. doi:10.1111/jop.12469
34. Verma A, Stellacci F. Effect of surface properties on nanoparticle–cell interactions. *Small*. 2010;6(1):12–21. doi:10.1002/smll.200901158
35. Hu R, Zheng L, Zhang T, et al. Molecular mechanism of hippocampal apoptosis of mice following exposure to titanium dioxide nanoparticles. *J Hazard Mater*. 2011;191(1–3):32–40. doi:10.1016/j.jhazmat.2011.04.027
36. Trouiller B, Reliene R, Westbrook A, Solaimani P, Schiestl RH. Titanium dioxide nanoparticles induce DNA damage and genetic instability in vivo in mice. *Cancer Res*. 2009;69(22):8784–8789. doi:10.1158/0008-5472.CAN-09-2496
37. Gui S, Zhang Z, Zheng L, et al. Molecular mechanism of kidney injury of mice caused by exposure to titanium dioxide nanoparticles. *J Hazard Mater*. 2011;195:365–370. doi:10.1016/j.jhazmat.2011.08.055
38. Moon C, Park HJ, Choi YH, Park EM, Castranova V, Kang JL. Pulmonary inflammation after intraperitoneal administration of ultrafine titanium dioxide (TiO₂) at rest or in lungs primed with lipopolysaccharide. *J Toxicol Environ Health A*. 2010;73(5):396–409. doi:10.1080/15287390903486543
39. Li N, Ma L, Wang J, et al. Interaction between nano-anatase TiO₂ and liver DNA from mice in vivo. *Nanoscale Res Lett*. 2009;5(1):108–115. doi:10.1007/s11671-009-9451-2
40. Mohammadi F, Sadeghi L, Mohammadi A, Tanwir F, Babadi VY, Izadnejad M. The effects of Nano titanium dioxide (TiO₂NPs) on lung tissue. *Bratisl Lek Listy*. 2015;116(6):363–367. doi:10.4149/bll_2015_069
41. Wang Y, Chen Z, Ba T, et al. Susceptibility of young and adult rats to the oral toxicity of titanium dioxide nanoparticles. *Small*. 2013;9(9–10):1742–1752. doi:10.1002/smll.201201185
42. Hong F, Wang L, Yu X, Zhou Y, Hong J, Sheng L. Toxicological effect of TiO₂ nanoparticle-induced myocarditis in mice. *Nanoscale Res Lett*. 2015;10(1):1029. doi:10.1186/s11671-015-1029-6
43. El-Sheikh A, Ameen S, Ibrahim H, Abdel-Fatah S. The immunotoxic effects of short term chronic exposure to Titanium Dioxide Nanoparticles on spleen of adult albino rats and the role of after toxic effect follow up. *AJFM*. 2016;26(1):115–128. doi:10.21608/AJFM.2016.18550
44. Senel S, Kremer M, Nagy K, Squier C. Delivery of bioactive peptides and proteins across oral (buccal) mucosa. *Curr Pharma Biotechnol*. 2001;2(2):175–186. doi:10.2174/1389201013378734